6A.1 EXPLORING THE IMPACT OF STORM RELATIVE HELICITY ON THE RELATIONSHIP BETWEEN COLD POOLS AND TORNADOES

Jason Naylor*
University of Louisville, Louisville, KY

1. INTRODUCTION

It is well known that the development of tornado-like vortices (herein simply referred to as tornadoes) in numerical simulations is sensitive to the structure and thermodynamic properties of the surface cold pool. [e.g., Snook and Xue 2008; Lerach et al. 2008; Lerach and Cotton 2012; Dawson et al. 2015]. These studies indicate that strong cold pools are associated with a weakening of the near surface circulation. This weakening is at least partially attributed to a horizontal displacement between the near-surface and midlevel circulations when cold air near the surface "surges" ahead of the midlevel updraft.

Naylor and Gilmore (2014a) simulated 19 tornadic and 14 nontornadic supercells with an idealized cloud model. Their analysis shows stronger cold pools in many of the tornado producing supercells compared to the nontornadic supercells at the time of tornadogenesis or tornadogenesis failure. Naylor and Gilmore (2014b) expanded on these results by repeating several of their tornadic simulations with a more sophisticated, double-moment microphysics parameterization. In all six environments, weakening the cold pool results in a weaker and shorter-lived tornado. This is in contrast to the studies mentioned above, as well as with observations that indicate tornadoes may be stronger when cold pools are relatively weak [e.g., Markowski et al. 2002].

The purpose of this study is to further explore the relationship between tornadoes and surface cold pools in numerical models and determine if that relationship is impacted by the amount of storm relative environmental helicity (SREH) in the initial sounding. Of particular interest is investigating if tornadoes that occur in environments with large SREH are less sensitive to changes in the surface cold pool than tornadoes in environments with smaller SREH.

* *Corresponding author address*: Jason Naylor, Department of Geography and Geosciences, University of Louisville, Louisville, KY, 40292. jason.naylor@louisville.edu

2. METHODOLOGY

Simulations were performed using version 18 of the CM1 cloud model. The model grid is configured with a horizontal domain of 120 km and a vertical domain of 20 km. A stretched grid is used in both the horizontal and vertical directions. The minimum horizontal grid spacing is 100 m and stretches to 400 m near the lateral boundaries. The vertical grid spacing is 50 m below 3 km, and stretches to 250 m from 3–6 km, with a constant spacing of 250 m above 6 km. Microphysical processes are parameterized using the single-moment scheme of Gilmore et al. (2004), and turbulence is parameterized using the so-called Smagorinsky scheme. Convection is initiated using the updraft nudging method described by Naylor and Gilmore (2012).

All simulations are initialized with the environment shown in Figure 1. This sounding is a 0-hr RUC-2 analysis sounding from the dataset of Thompson et al. (2007). It is associated with an F2 tornado that occurred near Cairo, IL on 18 September 2004. The original (control) hodograph is shown in Figure 2, along with modified hodographs for the SREH sensitivity experiments. The 0–3 km SREH in the control hodograph is 378 m^2 s^{-2}. The hodograph is varied by either amplifying the winds below 3 km to increase the SREH, or by straightening the hodograph to decrease the SREH. In these modified hodographs, SREH ranges from a maximum of 514 m^2 s^{-2} to a minimum of 210 m^2 s^{-2}.

To induce variations in cold pool structure, evaporation and melting rates within the microphysics parameterization were altered via a scaling parameter. A scaling value greater than 1 increases the evaporation and melting rates, resulting in larger magnitude deficits of pseudoequivalent potential temperature (θ_{ep}) in the surface cold pool. Scaling values less than 1 decrease the evaporation and melting rates, which leads to smaller magnitude θ_{ep} deficits.

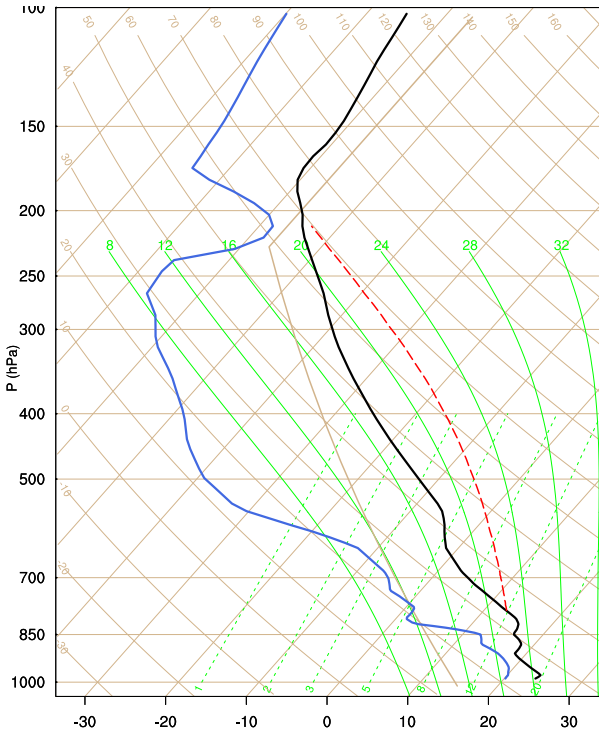

Fig 1. Skew-T showing the temperature and dew point profiles used to initialize all simulations.

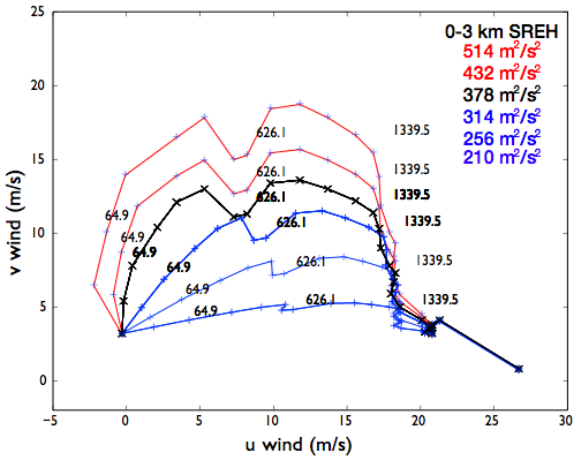

Fig 2. Hodograph showing the 0–6 km wind profiles for the various experiments. The original (control) hodograph is shown in black.

3. RESULTS

Values of 1.2, 1 (control), 0.85, and 0.5 were used to scale the evaporation and melting rates within the microphysics parameterization. Each of these scaling values is used in a simulation with one of the wind profiles shown in Figure 2, for a total of 24 simulations. A summary of tornado production within the current parameter space is shown in Table 1. All simulations with the control and enhanced SREH produce tornadoes, regardless of the strength of the surface cold pool—which is controlled by the evaporation and melting rates. As the hodograph is straightened and SREH is decreased, the simulations with the strongest melting/evaporation rates (and strongest cold pools) no longer produce tornadoes. In the smallest helicity environment, only the simulation with the weakest cold pool produces a tornado. Herein, only the seventeen tornado-producing simulations from Table 1 are analyzed.

The duration and intensity (as measured by minimum surface pressure) of the tornadoes in each simulation was examined and related to the characteristics of the surface cold pool. For this analysis, average and minimum θ_{ep} perturbations (relative to the base-state values) were calculated within a 400 m x 400 m box centered on the near surface circulation at *t*=2100 s. At this time, most simulations have a tornado present. The remaining simulations produce short-lived tornadoes (duration of 90 s or less) approximately 5–7 min prior. In general, smaller magnitude θ_{ep} deficits at *t*=2100 s are associated with stronger and longer-lived tornadoes (Figures 3, 4). Additionally, for a specific wind profile, decreasing the strength of the surface cold pool (via scaling the melting and evaporation rates) generally results in a stronger and longer-lived tornado, although there are specific instances when this is not true. For example, of the four simulations initialized with the largest SREH (scaled by 1.5), the strongest and longest-lived tornado occurs in the simulation with the largest magnitude θ_{ep} deficits. The strongest tornado in the control environment is also associated with relatively large θ_{ep} deficits.

All simulations cease tornado production by *t*=2600 s. In many of the simulations, this occurs coincident with cyclic mesocyclogenesis and a disruption of the midlevel updraft. Of the seventeen simulations that produce a tornado, nine experience cyclic mesocyclogenesis.

Table 1. Summary of tornado production within the tested parameter space. Simulations labeled "tor" produce a tornado, while "non" simulations do not. Bold numeric values on the x-axis represent the scaling parameter applied to the evaporation and melting rates within the microphysics, while the numbers on the y-axis represent the scaling applied to the 0–3 km winds in the initial environment.

Helicity \ LFO	**1.2**	**1**	**0.85**	**0.5**
1.5	tor	tor	tor	tor
1.2	tor	tor	tor	tor
1	tor	tor	tor	tor
0.8	non	non	tor	tor
0.5	non	non	tor	tor
0.2	non	non	non	tor

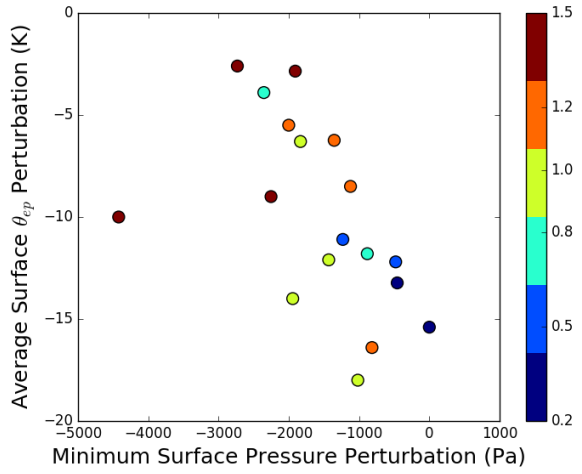

Fig 3. Scatterplot of average θ_{ep} perturbation (calculated in a 400 m x 400 m box surrounding the near surface circulation) at *t*=2100 s vs. minimum surface pressure associated with a tornado for each simulation. Points are colored by the SREH scaling parameter in the initial environment.

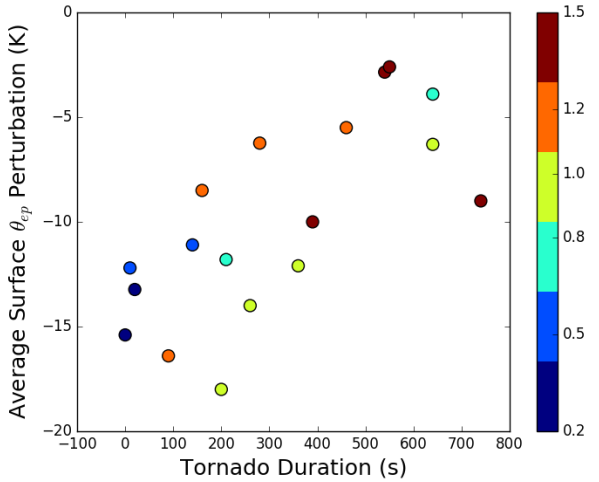

Fig 4. Same as 3, except showing tornado duration instead of minimum pressure.

In several other simulations, there is evidence that cyclic mesocyclogenesis initiates, but does not complete. All simulations show at least some indication of updraft weakening at midlevels between *t*=2400 s and *t*=3000 s. In the simulations with the two smallest SREH environments (scaling of 0.5 and 0.2), this weakening continues throughout the duration of the simulation. In all other simulations, the midlevel updraft eventually restrengthens and becomes quasi-steady.

A second tornado forms following the restrengthening of the updraft in four of the simulations. Three of these four are initialized with the control wind profile, while the fourth is initialized with slightly enhanced SREH (Table 2). None of the cases with reduced SREH produce a second tornado.

The four tornadoes that occur following midlevel updraft cycling were analyzed separate from the earlier tornadoes. A cold pool analysis, similar to that discussed previously, was performed at *t*=3600 s, when all four simulations contain a tornado (Figures 5,6). Although the number of points is small, a general trend emerges in the simulations of the control hodograph. In this environment, the strongest and longest-lived tornado that occurs after cyclic mesocyclogenesis is associated with the largest magnitude θ_{ep} deficits. Weakening the melting and evaporation results in progressively weaker and shorter-lived tornadoes.

Table 2: Same as Table 1, except showing simulations that produce a second tornado after updraft cycling (tor) and those that do not (non).

Helicity \ LFO	1.2	1	0.85	0.5
1.5	non	non	non	non
1.2	tor	non	non	non
1	tor	tor	tor	non
0.8			non	non
0.5			non	non
0.2				non

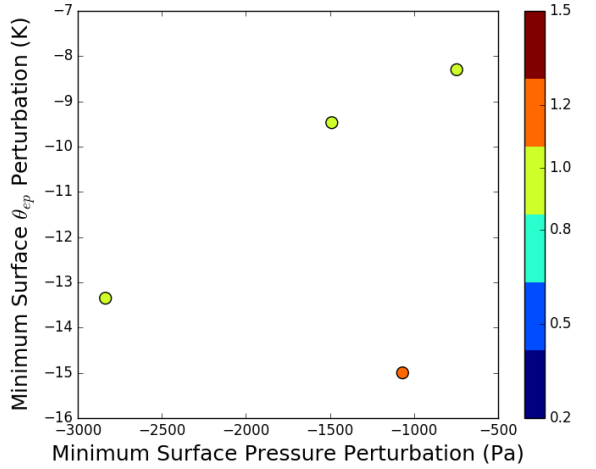

Fig 5. Same as 3, except at *t*=3600 s and only including simulations that produce a second tornado after updraft cycling.

In addition, cold pools in the simulations that are tornadic at *t*=3600 s tend to have larger magnitude θ_{ep} deficits surrounding the near-surface circulation than the cold pools in the nontornadic simulations at the same time (not shown).

It is also interesting that tornado development is relatively rare following updraft cycling. As mentioned previously, only four of the seventeen tornadic simulations produce a second tornado after updraft cycling, even though many of the

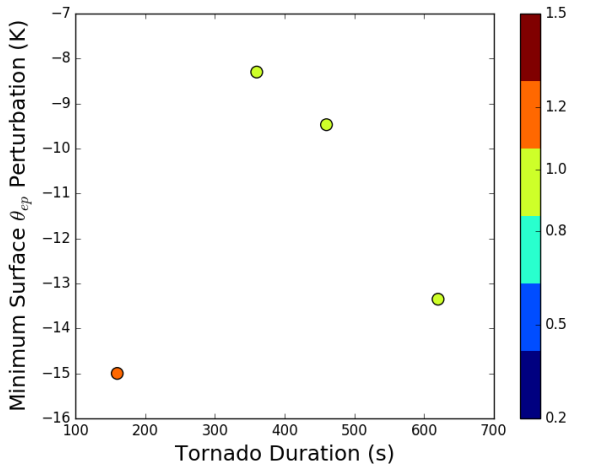

Fig 6. Same as 4, except at *t*=3600 s and only including simulations that produce a second tornado after updraft cycling.

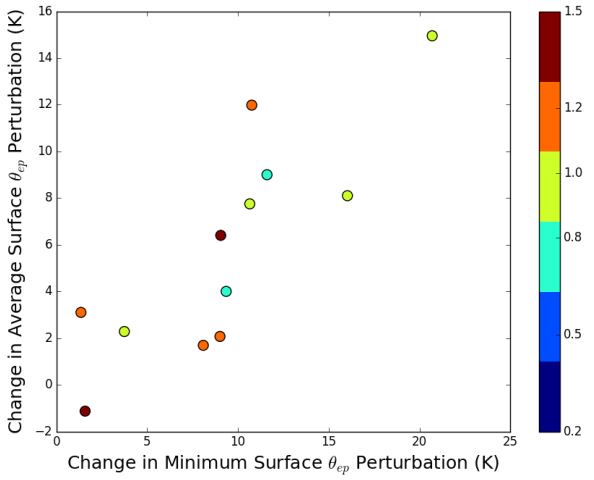

Fig 7. Scatterplot of the change in average θ_{ep} perturbation vs. change in minimum θ_{ep} perturbation from *t*=2100 s to *t*=3600 s. Points are colored by the amount of SREH in the initial environment.

supercells regain their strength and contain quasi-steady updrafts. This difference in tornado production may be related to changes in cold pool structure. In every simulation except one, cold pools are substantially weaker at *t*=3600 s than they are at *t*=2100 s (Figure 7). Additional analysis is needed to investigate the cause of this weakening as well as its impact on tornadogenesis in the simulations.

4. SUMMARY

All simulations with original or enhanced SREH produce a tornado, regardless of the properties of the surface cold pool. As SREH is decreased, the simulations with the strongest cold pools fail to produce tornadoes. This finding may suggest that tornado development is less sensitive to cold pool characteristics in large SREH environments than in environments with smaller SREH.

Although all of the simulations with the control or enhanced SREH produce tornadoes, there are considerable differences in duration and intensity. For a given environment, smaller θ_{ep} deficits within the surface cold pools generally correspond to stronger and longer-lived tornadoes; however there are a few specific examples were this is not the case. Furthermore, tornadoes that occur after updraft cycling seem to have the opposite association. In simulations of the control wind profile, large θ_{ep} deficits are associated with the strongest and longest-lived tornado that occurs after cyclic mesocyclogenesis. It is also found that θ_{ep} deficits become smaller over time in almost every simulation. Thus, cold pools are much stronger at *t*=2100 s, when tornadogenesis occurs in a number of the simulations, then at *t*=3600 s, when only a few simulations contain tornadoes. This may suggest that different mechanisms are at work for the later tornadoes, although trajectory analysis and vorticity budgets must be completed to investigate this idea further.

5. ACKNOWLEDGEMENTS

Thanks to George Bryan for his continual development of CM1. Resources from the Extreme Scientific and Engineering Discovery Environment (XSEDE) were used for all numerical simulations. Travel support was provided by the University of Louisville.

REFERENCES

Dawson, D. T. II, M. Xue, J. A. Milbrandt, and A. Shapiro, 2015: Sensitivity of real-data simulations of the 3 May 1999 Oklahoma City tornadic supercell and associated tornadoes to multimoment microphysics. Part I: Storm- and tornado-scale numerical forecasts. *Mon. Wea. Rev.*, **143**, 2241– 2265.

Gilmore, M. S., J. M. Straka, and E. N. Rasmussen, 2004: Precipitation and evolution sensitivity in simulated deep convective storms: Comparisons between liquid-only and simple ice and liquid phase microphysics. *Mon. Wea. Rev.*, **132**, 1897-1916.

Lerach, D. G., B. J. Gaudet, and W. R. Cotton, 2008: Idealized simulations of aerosol influences on tornadogenesis. *Geophys. Res. Lett*., **35**, L23806.

Lerach, D. G., and W. R. Cotton, 2012: Comparing aerosol and low-level moisture influences on supercell tornadogenesis: Three-dimensional idealized simulations. *J. Atmos. Sci*., **69**, 969-987.

Markowski, P. M., E. N. Rasmussen, and J. M. Straka, 2002: Direct thermodynamic observations within the rear-flank downdrafts of nontornadic and tornadic supercells. *Mon. Wea. Rev.*, **130**, 1692- 1721.

Naylor, J. and M. S. Gilmore, 2012: Convective initiation in an idealized cloud model using an updraft nudging technique. *Mon. Wea. Rev.*, **140**, 3699–3705.

Naylor, J. and M. S. Gilmore, 2014a: Vorticity evolution leading to tornadogenesis and tornadogenesis failure in simulated supercells. *J. Atmos. Sci.*, **71**, 1201–1217.

Naylor, J. and M. S. Gilmore, 2014b: Tornadogenesis and tornadogenesis failure in simulated supercells. *27th Conf. on Severe Local Storms*, Madison, WI, Amer. Meteor. Soc.

Snook, N., and M. Xue , 2008: Effects of microphysical drop size distribution on tornadogenesis in supercell thunderstorms. *Geophys. Res. Lett.*, **35**, L24803.

Thompson, R. L., C. M. Mead, and R. Edwards, 2007: Effective storm-relative helicity and bulk shear in supercell thunderstorm environments. *Wea. Forecasting*, **22**, 102-115.